Observations of Water Monomers in Supersaturated $NaClO_4$, $LiClO_4$, and $Mg(ClO_4)_2$ Droplets Using Raman Spectroscopy

Yun-Hong Zhang[†,‡] and Chak K. Chan*[,†]

Department of Chemical Engineering, Hong Kong University of Science and Technology, Clear Water Bay, Hong Kong, China, and Department of Chemistry, School of Science, Beijing Institute of Technology, Beijing 100081, China

Received: October 3, 2002; In Final Form: March 11, 2003

Salts of the same anions of Mg^{2+}, Na^+, and Li^+ have been found to exhibit different hygroscopic properties. These differences are attributed to the molecular structural properties of the hydrogen bonding network of the water molecules in the second and first hydrated layers of Mg^{2+}, Na^+, and Li^+. To study the structures of water molecules, in particular, the presence of water monomers, Raman spectra of single levitated droplets of aqueous $NaClO_4$, $LiClO_4$, and $Mg(ClO_4)_2$ solutions from diluted concentrations to high supersaturations were measured. Because heterogeneous nucleation was suppressed in these levitated droplets, supersaturated droplets with a water-to-solute ratio (WSR) as low as 2 was achieved. Taking advantage of the structure breaking effect of ClO_4^- on the hydrogen bonding network of water molecules, Raman spectra of water monomers in these highly supersaturated droplets were observed. At a low WSR, two peaks at 3549 and 3588 cm^{-1} for water monomers with one and two weak hydrogen bonds with ClO_4^- were observed for $NaClO_4$ droplets. Compared with those of the $NaClO_4$ droplets, the peaks of the water monomers in supersaturated $LiClO_4$ and $Mg(ClO_4)_2$ droplets red-shifted to 3553 and 3546 cm^{-1}, respectively. This observation is consistent with the order of the increase of the polarization effect of the cations, i.e., $Na^+ < Li^+ < Mg^{2+}$. The intensity ratios of the strongly hydrogen-bonded components to the water monomers, i.e., I_{3440}/I_{3549} and I_{3289}/I_{3549} for $NaClO_4$, I_{3455}/I_{3553} and I_{3275}/I_{3553} for $LiClO_4$, and I_{3411}/I_{3546} and I_{3440}/I_{3549} for $Mg(ClO_4)_2$, were used to study the effects of the presence of ClO_4^- on the water structures of the hydration layers of Na^+, Li^+, and Mg^{2+}. The results were explained in terms of the stability of water molecules in the inner spheres of these hydrated cations.

I. Introduction

Hygroscopicity is one of the most important properties of atmospheric aerosols. Aerosols change their size and concentrations through absorbing water with increasing relative humidity (RH) or evaporating water with decreasing RH. Such processes affect the size distributions, radiative properties, deposition characteristics, and chemical reactivity of the aerosols.[1] Na^+ and Mg^{2+} are the major cations in sea-salt aerosols. However, their salts of the same anions have very different hygroscopic properties.[2,3] On a molecular level, the water content of an aerosol is controlled by the interactions between the water molecules and the solutes, including the hydration of ions, the formation of ion pairs and contact ion pairs, as well as the hydrogen bonding between water molecules.

Previously, when we coupled a single particle levitation system with a Raman spectroscopic system, we showed that the Raman spectra of aqueous sulfate droplets can be used to correlate the changes of molecular structures, the formation of contact ion pairs in particular, with their hygroscopic properties.[4,5] This technique facilitates the study of extremely supersaturated solutions, in which the interactions between solute and water molecules are much more extensive than in a typical bulk study. This study examines the interactions between water molecules and solutes, especially under the supersaturated state.

Although water molecules have a simple structure, there are very complex hydrogen-bond interactions in bulk liquid. Vibrational spectroscopy, i.e., FTIR or Raman spectroscopy, has been used extensively to study the structures of bulk aqueous solutions because the O−H stretching vibrations are sensitive to the interactions between the water molecules and the hydrated ions, the hydrogen bonds between water molecules, as well as the effects of ions on the hydrogen bonds.[6−20] These studies include the effects of temperature or the effects of the concentration of various ions on the envelope of the O−H stretching vibration,[8−14] on the structures of hydrogen bonding in liquid water above the critical point,[15,16] and on the structures of water in the glassy state of some aqueous inorganic salt solutions.[17,18] In particular, Kanno et al.[18] have observed the existence of water monomers in glassy aqueous $Ca(ClO_4)_2$ solutions at the temperature of liquid nitrogen. There are also a number of studies on gaseous water clusters carried out with the use of terahertz laser vibration−rotation-tunneling spectra and mid-laser spectra, from which the molecular structures of various water clusters (dimer through hexamer) are analyzed in conjunction with new theoretical advances.[6] Furthermore, surface enhanced Raman scattering (SERS) of water on specific electrodes has made it possible to obtain the structural information on the interaction between water molecules and ions on electrodes.[20] Although there are many reports on the hydrogen bonding of water in the literature, an accurate description of liquid water has not been available. [6,7]

ClO_4^- ions have a slight capability to form hydrogen bonds with water molecules and are therefore considered as "structure

* To whom correspondence should be addressed. E-Mail: keckchan@ust.hk. Phone: (852) 2358-7124. Fax: (852) 2358-0054.
† Hong Kong University of Science and Technology.
‡ Beijing Institute of Technology.

10.1021/jp0271256 CCC: $25.00
Published on Web 07/12/2003

breaking" ions that destroy the hydrogen bond network between water molecules.[8,9] Combining Raman spectroscopy and the electrodynamic balance (EDB) technique, we report the first observation of the O−H stretching vibration band related to water monomers in aqueous $NaClO_4$, $Mg(ClO_4)_2$, and $LiClO_4$ solutions at room temperature. In this paper, the ability of ClO_4^- to break the hydrogen bonds in the inner sphere of the hydrated Mg^{2+}, Na^+, and Li^+ perchlorate droplets will be discussed.

II. Experimental Section

The electrodynamic balance (EDB) has been used extensively to study the hygroscopic properties of single droplets of inorganic salts, organic salts, and organic acids.[21] One of the advantages of the EDB technique is that a droplet can be freely levitated in an electric field in an EDB. Thus, heterogeneous nucleation is suppressed and therefore the droplets usually achieve the supersaturated state before crystallization, if it occurs. We have studied the formation of contact ion pairs of sulfate salts in highly supersaturated concentrations by coupling the EDB with a Raman spectroscopic system. This cannot be achieved in bulk solutions.[4,5]

The experimental setup and procedures used in this study were identical to those used in Zhang and Chan.[4,5] In this paper, we will briefly describe the operational principle of the EDB here. It consisted of a pair of DC endcap electrodes and an AC ring electrode. The high voltage AC electrode was used to trap a single charged droplet oscillating around the center of the balance. When the electrostatic force experienced by the particle balanced its weight, the particle was stationary at the center of the EDB. Hence, the applied balancing DC voltage was proportional to the mass of the levitated particle. When the ambient RH was changed, the particle achieved equilibrium with the gas phase by absorbing an appropriate amount of water. The molar water-to-solute ratio (WSR) of the droplet was determined by the DC balancing voltage measurements. The WSR of the droplets at an equilibrium RH value were determined using an anhydrous $NaClO_4$ solid particle, crystal $LiClO_4 \cdot 3H_2O$ and $Mg(ClO_4)_2 \cdot 6H_2O$ as the reference states. The air flow for controlling the RH in the EDB was momentarily stopped when the balancing voltage was measured. The RH was determined by a dew-point hygrometer (EG&G DewPrime model 2000).

A Raman system, consisting of a 5 W argon ion laser (Coherent I90−5) and a 0.5 m monochromator (Acton SpectraPro500) attached to a CCD detector (Princeton Instrument, TE/CCD-1100PFUV), was incorporated into the EDB system. The 514.5 nm line of an argon-ion laser with an output power between 0.5 and 1 W was used as the source of excitation. A pair of lenses, which matches the f/6.9 optics of the monochromator, was used to focus the 90° scattering of the levitated droplet on the slit (100 μm) of the monochromator. A 514.5 nm Raman notch filter was placed between the two lenses to remove the strong Rayleigh scattering. A 300 g/mm grating of the monochromator was selected. The resolution of the spectra obtained was about 10 cm^{-1}. All measurements were made at ambient temperatures of 22−24 °C. The integration time of each spectrum was 1 s. Typically, an average of 50 spectra were used to produce a spectrum of a droplet at each RH.

Because the O−H stretching band is a broadband emission, morphological dependent resonances (MDR) of Mie scattering appear in the Raman spectra of water.[22] To increase the Raman signal and suppress the MDR effects, large droplets (diameter > 60 μm) were selectively trapped by applying a high frequency (18.5 kHz) and a high intensity (1200 V) AC to the AC electrode. Even though the isotropic spectra of water have been used widely to study water structures, it is not easy to obtain the isotropic spectra of the droplets because of the intensity fluctuation due to the MDR effects.

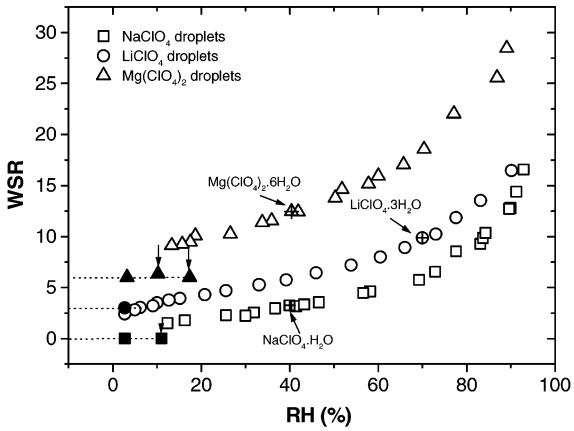

Figure 1. Water-to-solute molar ratio (WSR) of $NaClO_4$ droplets (□) $LiClO_4$ droplets (○) and $Mg(ClO_4)_2$ droplets (△) at various relative humidities (RH). Solid symbols indicate the solid particles after crystallization. The symbols with a plus sign indicate saturation points of the thermodynamically stable solid phase in bulk solutions.

III. Results and Discussion

A. Hygroscopicity of $NaClO_4$, $LiClO_4$, and $Mg(ClO_4)_2$. Figure 1 shows the hygroscopic properties of $NaClO_4$ (open squares), $LiClO_4$ (open circles), and $Mg(ClO_4)_2$ (open triangles) droplets in terms of equilibrium molar WSR as a function of decreasing RH. Efflorescence, which resulted in a sudden decrease in the WSR, was observed at about RH = 11% for $NaClO_4$ (the solid squares), which was much lower than the saturation point of $NaClO_4 \cdot H_2O$ (WSR = 3.24, corresponding to the open square with a plus sign in Figure 1).[23] An extremely low WSR of 1.6 was achieved before crystallization occurred. At this low WSR, one Na^+ and one ClO_4^- shared less than two water molecules. The possibility of water molecules forming a hydrogen bond between themselves was significantly reduced when compared with bulk samples. It is interesting to note that a $NaClO_4$ droplet crystallized at RH = 10% to form an anhydrous particle rather than the most thermodynamically stable state of the $NaClO_4 \cdot H_2O$ monohydrate.

For lithium perchlorate, a mixture including the most stable $LiClO_4 \cdot 3H_2O$ and another metastable solid phase was formed until the particle was dried at RH = 3% for about 10 h. Upon further drying, there was a DC voltage increase and the metastable phase was finally transformed to $LiClO_4 \cdot 3H_2O$ (the solid circle), which was selected as the reference state for WSR calculations. Again, the WSR of the $LiClO_4$ droplets achieved was as low as 2.8 without crystallization, which was much lower than its respective saturation value at WSR = 9.46 for $LiClO_4 \cdot 3H_2O$ (the open circle with a plus).[23] It is interesting to note that $LiClO_4 \cdot 3H_2O$ can be formed from a supersaturated solution with a WSR less than 3.

Unlike $NaClO_4$, magnesium perchlorate crystallized at RH = 10−18% to form the most stable $Mg(ClO_4)_2 \cdot 6H_2O$ (solid triangles). Corroborative spectroscopic evidence will be shown later. The lowest WSR achieved for the supersaturated droplets of magnesium perchlorate was 9.1, which is lower than the saturation value (WSR = 12.46, the open triangle with a plus sign).[23]

B. Stretching Vibration Band of Water (ν_{O-H}) in Aqueous Droplets. Figure 2 shows a comparison of the spectral

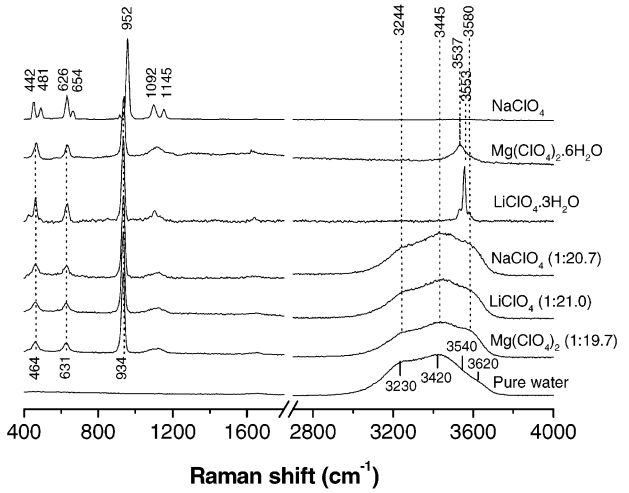

Figure 2. Raman spectra of crystalline $NaClO_4$, $LiClO_4$, and $Mg(ClO_4)_2$ and their bulk solutions and pure water.

characteristics of υ_{O-H} of pure water with those of the bulk solutions and solids. In pure liquid water, the O−H stretching envelope is generally composed of four components, attributed to an ice-like component (C_1) at ∼3230 cm^{-1}, an ice-like liquid component (C_2) at ∼3420 cm^{-1}, a liquidlike amorphous phase (C_3) at ∼3540 cm^{-1}, and monomeric H_2O (C_4) at 3620 cm^{-1}, as shown in Figure 2.[8,15] Bulk aqueous $NaClO_4$, $LiClO_4$, and $Mg(ClO_4)_2$ solutions (ClO_4^-/H_2O of about 1:20) have a similar envelope of the O−H stretching band. In addition, a main peak at ∼3445 cm^{-1} and two shoulders at ∼3244 and ∼3580 cm^{-1} were observed. There were small spectral differences in the bulk solutions of perchlorate of Na^+, Li^+, and Mg^{2+}. However, the presence of ClO_4^- in the solutions increased the intensity ratio at 3580 cm^{-1} to that at ∼3445 cm^{-1} , when compared with the ratio of pure water. This is the result of the structure breaking effect of ClO_4^- on the hydrogen bonds between the water molecules.[8,9] The O−H stretching vibration bands of crystalline $LiClO_4 \cdot 3H_2O$ and $Mg(ClO_4)_2 \cdot 6H_2O$ at 3553 and 3537 cm^{-1}, respectively, were observed. Solid $NaClO_4$ did not have any O−H stretching vibration band, as expected.

The Raman spectra of $NaClO_4$, $LiClO_4$, and $Mg(ClO_4)_2$ droplets at different WSR are shown in Figure 3a−c. The spectra were normalized with the intensity of the ClO_4^- symmetric stretching band (υ_1 at ∼934 cm^{-1}). The dotted lines at ∼3230, ∼3420, ∼3540, and ∼3620 cm^{-1} in Figure 3 are the fitting peak positions of the four components of pure water.[8,15]

In the $NaClO_4$ droplets at WSR = 16.6, the maximum peak of the O−H stretching vibration appeared at 3440 cm^{-1} (C_2) (Figure 3a). There were two shoulders near 3289 (C_1) and 3588 cm^{-1} (C_3 + monomers). As the WSR decreased during droplet evaporation, the intensity of the water O−H stretching vibration envelope decreased with a more significant reduction on the lower frequency side, indicating a faster decrease in the contributions of the C_1 and C_2 components. At WSR = 12.7, the intensities at 3440 and 3588 cm^{-1} were similar. As the WSR further decreased to 9.8, a peak appeared at 3549 cm^{-1} and the original peak at 3440 cm^{-1} became a shoulder. Most interestingly, at WSR = 1.6, the shoulder at 3289 cm^{-1} disappeared and the shoulder at 3440 cm^{-1} made small contributions to the O−H stretching band as shown in Figure 4. The residual O−H stretching envelope had a narrow full width at half-height (fwhh) (132 cm^{-1}), compared with that of the dilute droplets (378 cm^{-1} for WSR = 16.6). It seems that such envelope is composed of two components with peaks at 3549 and 3588 cm^{-1}. No peak was observed in the O−H stretching region for the solid particle,

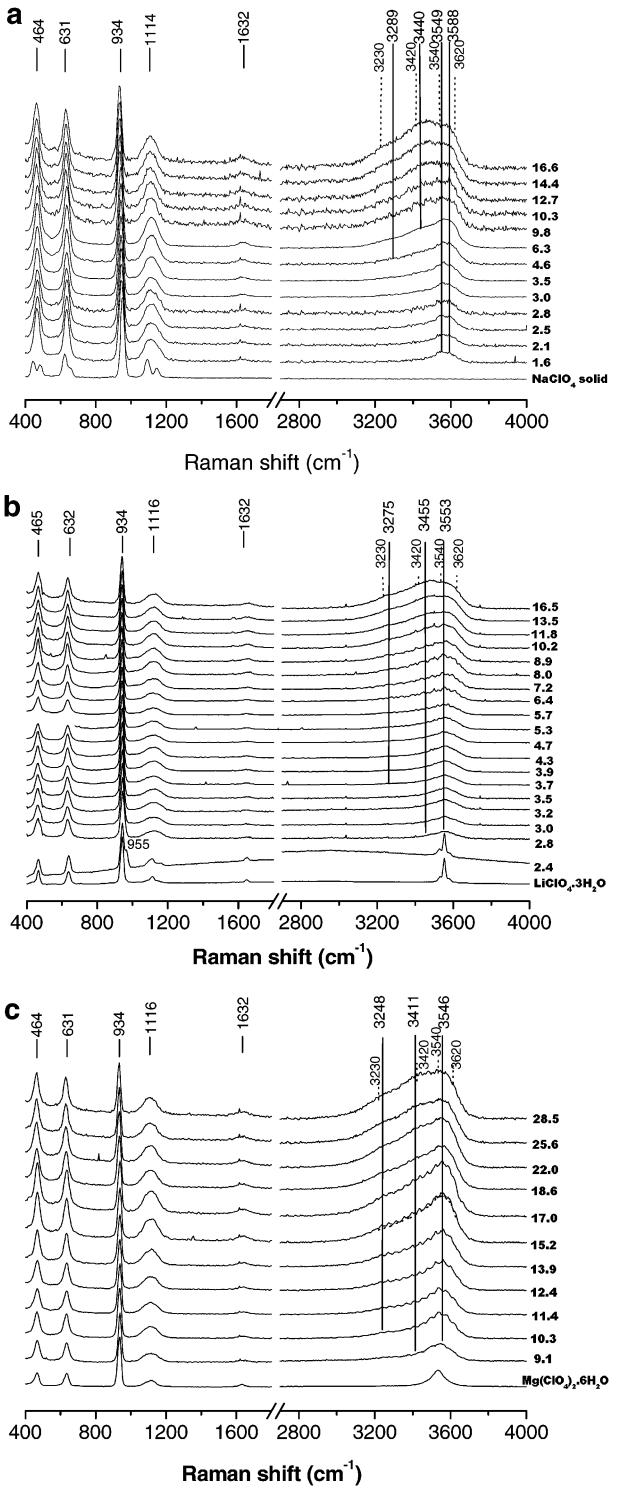

Figure 3. Raman spectra of single droplets of (a) aqueous $NaClO_4$ solutions, (b) aqueous $LiClO_4$ solutions, and (c) aqueous $Mg(ClO_4)_2$ solutions at various WSR.

indicating that anhydrous $NaClO_4$, instead of the most thermodynamically stable $NaClO_4 \cdot H_2O$, was formed, as shown in Figure 1.

Shown in Figure 3b are the Raman spectra of the $LiClO_4$ droplets as a function of WSR. The maximum intensity of the main peak appeared at ∼3455 cm^{-1} (C_2) and two shoulders were resolved at ∼3275 (C_1) and ∼3553 cm^{-1} (C_3 + monomers) in the diluted droplet (WSR = 16.5) similar to that of the $NaClO_4$ droplet with WSR of 16.6. As the WSR decreased, the intensity of the 3455 cm^{-1} peak and the 3275 cm^{-1} shoulder

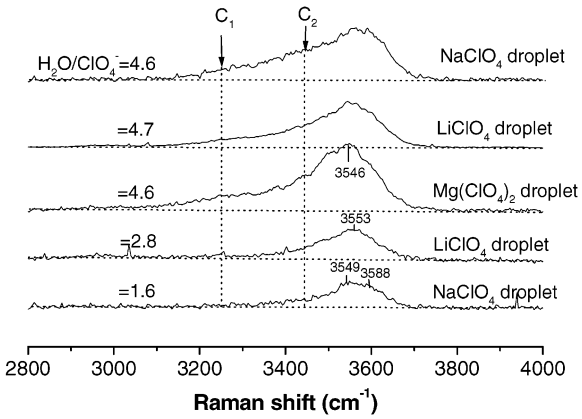

Figure 4. Resolved υ_{O-H} bands of the water monomers in supersaturated droplets.

decreased more than that of ~3553 cm^{-1}. The contribution of the shoulder at 3275 cm^{-1} approached zero at WSR = 2.8, as shown in Figure 4. Furthermore, the fwhh decreased from 381 to 146 cm^{-1} as the WSR decreased from 16.5 to 2.8. Morphology-dependent resonances were observed, especially at WSR between 11.3 and 5.8. A solid particle was formed when a stream of dry air was introduced into the EDB for about 10 h. A sharp band at 3553 cm^{-1} and four bands at 463, 363, 935, and 1094 cm^{-1} were observed in the spectrum of the dry particle, similar to that of the bulk solid $LiClO_4 \cdot 3H_2O$ in Figure 2, indicating that the main component of the particle is $LiClO_4 \cdot 3H_2O$. A shoulder at 956 cm^{-1} was also observed, which may be related to a metaphase in the formation of the dried particle. This change in the Raman spectrum is consistent with the small DC increase with further drying shown in Figure 1. Both are the results of the conversion of the metaphase to $LiClO_4 \cdot 3H_2O$. Therefore, we selected $LiClO_4 \cdot 3H_2O$ as the reference state for the calculations of WSR.

Figure 3c shows that at WSR = 28.5, equivalent to a molar ratio of 14.3 between H_2O and ClO_4^-, the main peak in the water stretching region of $Mg(ClO_4)_2$ droplets appeared near 3546 cm^{-1} (C_3 + monomers). The two shoulders on the lower wavenumber side appeared at ~3248 (C_1) and ~3411 cm^{-1} (C_2), respectively. Similar to the case of $NaClO_4$, the reductions in the intensities of these two shoulders were more pronounced than that of the main peak at decreasing WSR. Nevertheless, these two shoulders existed even at WSR = 9.1, corresponding to a molar ratio of water to perchlorate of about 4.6 (see Figure 4). The fwhh decreased from 396 to 183 cm^{-1} as the WSR decreased from 28.5 to 9.1. The solid particle formed after crystallization is indeed $Mg(ClO_4)_2 \cdot 6H_2O$, based on the reference spectrum of crystalline $Mg(ClO_4)_2 \cdot 6H_2O$ shown in Figure 2. The water molecules in the $Mg(ClO_4)_2 \cdot 6H_2O$ particle gave a symmetric peak at 3537 cm^{-1} with a fwhh of 82 cm^{-1}. The small sharp peaks superimposed onto the envelope of the broad water stretching band, especially for the droplet of WSR between 17.0 and 10.3, were attributed to the morphology-dependent resonance of the droplets.

C. Vibrational Modes of ClO_4^- and the Formation of Contact Ion Pairs. In the spectra of the bulk aqueous solutions of $NaClO_4$, $LiClO_4$, and $Mg(ClO_4)_2$ shown in Figure 2, the four bands at ~464, ~631, ~934, and ~1116 cm^{-1} are signatures corresponding to the two bending vibration modes (υ_2, E, R; υ_4, F_2, IR, R) and the symmetric and asymmetric stretching vibration modes (υ_1, A_1, R; υ_3, F_2, IR, R) of the hydrated unperturbed perchlorate anion with T_d symmetry. The notations IR and R denote infrared and Raman activities, respectively. Seven bands, not found in the spectrum of the bulk aqueous $NaClO_4$ solutions, were resolved for solid $NaClO_4$. Klassen et al.[24] and Miller and Macklin[25] have attributed such spectral differences to the symmetric change from T_d of free ClO_4^- in solutions to D_{2h1} in crystals where strong interactions between Na^+ and ClO_4^- exist. In contrast, direct interactions between Li^+ and ClO_4^- and between Mg^{2+} and ClO_4^- cannot exist in the crystalline hydrates of $LiClO_4 \cdot 3H_2O$ and $Mg(ClO_4)_2 \cdot 6H_2O$ because of the presence of the hydration water. Thus, the Raman spectra of $LiClO_4 \cdot 3H_2O$ and $Mg(ClO_4)_2 \cdot 6H_2O$ were very similar to those of their bulk solutions.

Figure 5 shows the changes of the υ_1 band of (a) $NaClO_4$, (b) $LiClO_4$, and (c) $Mg(ClO_4)_2$ as a function of the WSR. In $NaClO_4$ droplets, a blue-shift from 934 to 944 cm^{-1} was found when the WSR decreased to 1.6. Such spectral change has been attributed to the transformation of free perchlorate ions to solvent separated ion pairs (peak at 938 cm^{-1}) and then to the contact ion pairs (peak at 943 cm^{-1}) of Na^+ and ClO_4^-.[25,26] Frost et al.[26] have estimated that the molar fractions of contact ion pairs and solvent-separated ion pairs in 8 mol L^{-1} bulk $NaClO_4$ solutions (WSR = 7) are 0.15 and 0.64, respectively, with the remaining fraction being free ions. In saturated bulk $NaClO_4$ solutions (WSR = 3.24), the molar fraction of contact ion pairs increases to 0.545.[25] Even though we cannot accurately determine the fractions of each component because of the limitation of spectral resolution, it can be expected that the solvent-separated ion pairs and contact ion pairs were the main components when the WSR was between 6.3 and 1.6. For $LiClO_4$ droplets, there was a small blue-shift from 934 to 938 cm^{-1} when the WSR approached 6.4, which is consistent with the literature that only a small amount of solvent-separated ion pairs (molar fraction of 0.1) exist in 5 mol L^{-1} $LiClO_4$ solutions.[26] In the $LiClO_4 \cdot 3H_2O$ crystals, Li^+ is hydrated with six water oxygen atoms by a face-sharing octahedral of $Li(H_2O)_6^+$.[27,28] Thus, Li^+ salts tend to be more hydrated and thus more hygroscopic than Na^+ salts, as presented in Figure 1. For $Mg(ClO_4)_2$ droplets, the υ_1 band shifted from 934 to 939 cm^{-1} as the WSR decreased to 18.6. Considering the differences of the hydration energy and the radius between Na^+, Li^+, and Mg^{2+} shown in Table 1, Li^+ and Mg^{2+} tend to be hydrated and do not form contact ion pairs even in supersaturated droplets. However, contact ion pairs between Li^+ and ClO_4^- were formed in the metastable solid phase, as indicated by the shoulder at 955 cm^{-1} shown in Figure 5b. This metastable phase was strongly hygroscopic and transformed into $LiClO_4 \cdot 3H_2O$ by absorbing water even at very low relative humidity (3%). Overall, it was found that the higher the tendency of the salt to form contact ion pairs, the less hygroscopic it is.

D. Water Monomers in Supersaturated Solutions. There are some Raman studies of the effect of ClO_4^- on the structure of the hydrogen bonding network of aqueous solutions.[8,9] The water envelope of the diluted aqueous $NaClO_4$ droplets is similar to that of bulk $NaClO_4$ solutions.[8,9] The steep decrease in the intensity on the low wavenumber side of the O−H stretching vibration results from the "structure breaking" effect of ClO_4^-. In supersaturated droplets in which the contributions of the C_1 and C_2 components (at 3289 and 3440 cm^{-1}, respectively) were small, the effect of ClO_4^- became more pronounced. For example, the C_1 component almost disappeared when the WSR of the $NaClO_4$ droplets approached 1.6, as shown in Figure 4. Although a band corresponding to the pure water monomer component (C_4) of pure liquid water at 3620 cm^{-1} was not observed, the two residual O−H stretching bands at 3549 and 3588 cm^{-1} are an indirect evidence of the presence of the water monomers connected with the ClO_4^- anions by weak hydrogen

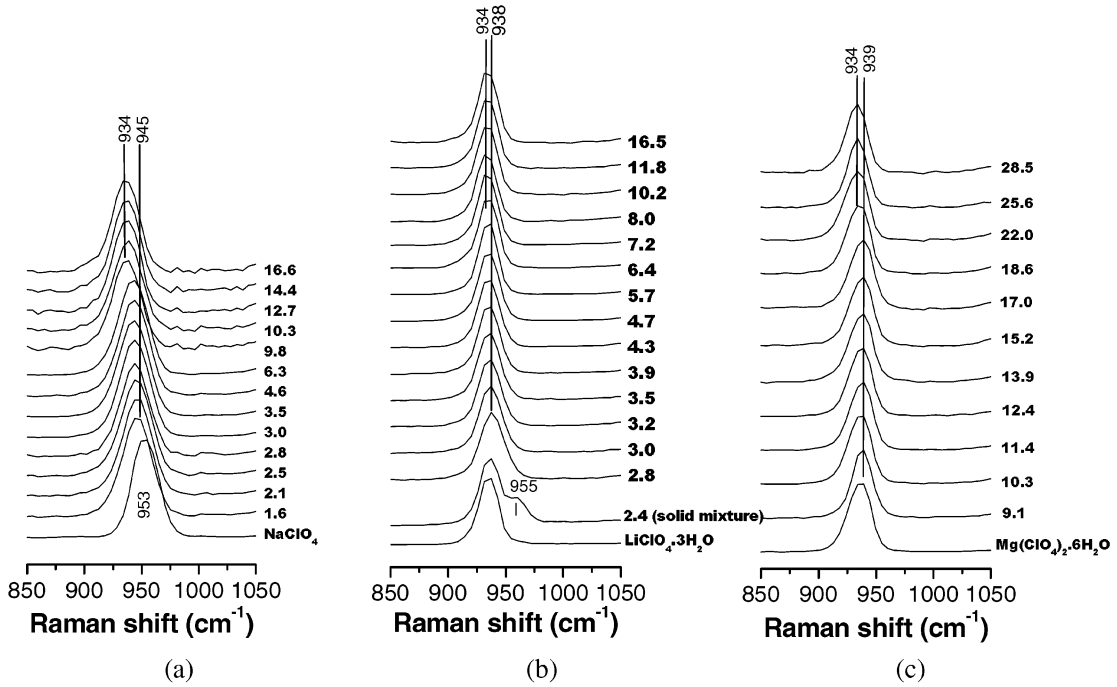

Figure 5. v_1 vibration bands of single droplets of (a) aqueous $NaClO_4$ solutions, (b) aqueous $LiClO_4$ solutions, and (c) aqueous $Mg(ClO_4)_2$ solutions at various WSR.

TABLE 1: Hydration Properties of the Cations[32,33]

parameters	Na^+	Li^+	Mg^{2+}
ionic radius (Å)	0.95	0.60	0.64
distance of $M-O(H_2O)_6$	2.40−2.50	1.95−2.18	2.00−2.15
hydration energy (kJ mol^{-1})	−405.4	−514.1	−1922.1
hydration water number			
(XRD)[32b]	4−6	4−6	6
(NMR)[32c]	3−4.6	3.4−5	6
(transference numbers)[32d]	7−9	13−14	24−28
	13	22	12−14
(ionic mobility)[32e]	5−10	7−21	
	3	2	9
	6	8	11
residence time of a water molecule in the first layer ($\times 10^{-12}$ s)[34]			
(MD)[a]	9.9	33	
(NMR)		∼30	2×10^6

[a] MD = molecular dynamic stimulation.

bonds. Kanno et al.[18] have observed the trapezoidal Raman peaks at 3585 and 3545 cm^{-1} in glassy aqueous $Ca(ClO_4)_2$ solutions at low temperatures. They attributed these two peaks to the v_1 mode of H_2O molecules with one and two weak hydrogen bonds. Joeston and Drago [29] have estimated that a weak interference of 1 kcal mol^{-1} with the O−H stretching mode is sufficient to lower the v_{O-H} symmetric stretching frequency at 3650 cm^{-1} (the symmetric stretching frequency of water vapor) by 60 cm^{-1}. The energy of the weak hydrogen bonds between the water monomers and the ClO_4^- ions is about 1∼2 kcal mol^{-1},[29] which is much smaller than the energy of the fully hydrogen-bonded liquid waters (C_1 component, about 7 kcal mol^{-1}). Thus, the peaks at 3588 and 3549 cm^{-1} observed in the supersaturated droplets were assigned to the water monomers that were weakly hydrogen-bonded with ClO_4^- ions.

In Figure 4, the resolved peak positions of the water monomers appear at ∼3553 and ∼3546 cm^{-1} for $LiClO_4$ droplets at WSR = 4.6 and $Mg(ClO_4)_2$ droplets at WSR = 9.1, respectively. The effects of Mg^{2+}, Na^+, and Li^+ on the shift in the v_{O-H} band in the half-water (DOH) complexes of I^- in some organic solvents measured by IR spectroscopy have been reported.[30,31] The v_{O-H} band of the monomers shifts from 3450 cm^{-1} in the complex of [DOH···I^-] to 3440 cm^{-1} in [Na^+···DOH···I^-], to 3420 cm^{-1} in [Li^+···DOH···I^-], and to 3350 cm^{-1} in [Mg^{2+}···DOH···I^-]. In this study, we have observed a similar trend although the shifts were smaller. The larger effects reported in the literature may be explained by the stronger interactions between water and cations in these complexes formed in the special organic solvents used by the researchers.

E. Structure of Water of the Inner Sphere and the Second Layer. Table 1 shows the hydration properties of Na^+, Li^+, and Mg^{2+}. There are considerable differences in the hydration numbers determined by different methods, even for the same ion.[32] Results reported by various investigators using the same technique also showed significant differences. The variation of the values for each of these ions is much larger than the experimental uncertainty. This suggests that gross inconsistencies exist in the assumptions or interpretations or that the different techniques are in fact measuring different parameters. All in all, there is a lack of understanding of the hydrogen bonding network in the first and second hydration layers of metal ions on a molecular level.

The most direct approach to investigating the hydrogen bonds between water molecules and between water and anions is to obtain the vibration spectra below 500 cm^{-1}. However, the strong quasielastic Rayleigh wing, extending to 500 cm^{-1}, complicates the detection of the weak low-frequency modes of the hydrogen bonds. Recently, Rudolph and co-workers[33] studied the hydration process of Li^+ and Mg^{2+} with the combination of Raman spectroscopy and ab initio quantum chemistry calculations. In particular, they studied the low-frequency Li−O modes of $Li(OH_2)_n^+$ and the Mg−O modes of $Mg(OH_2)_n^{2+}$ by the normalization of the low-frequency Raman data, taking into consideration the Bose-Einstein temperature factor and a frequency factor. Hydrogen bonds between $Li^+-OH_2\cdots X$ (X = OH_2, Cl^-, Br^-) were resolved as a function of the

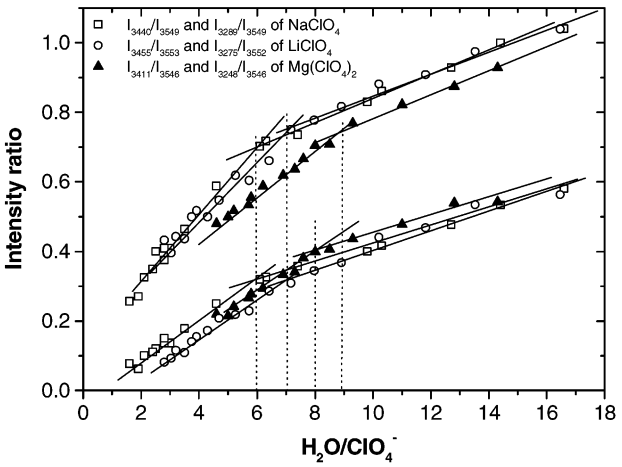

Figure 6. Relative intensity ratios of the two shoulders at the lower wavenumber side (C_1 and C_2) and the main peak (water monomers) at various H_2O/ClO_4^- molar ratios.

concentration of the salts. In our experiments, it is not possible to obtain the isotropic spectra and the Raman signals of the droplets were too weak for the observation of these bands as mentioned above. However, the O−H stretching band is useful to study the first and second hydration layers, especially in supersaturated solutions.

The O−H stretching vibration spectra of water molecules at WSR between 16.6 and 1.6 for $NaClO_4$ droplets, between 16.4 and 2.8 for $LiClO_4$ droplets, and between 28.7 and 9.1 for $Mg(ClO_4)_2$ droplets were shown in Figure 3. At these WSR, the envelope of the O−H stretching vibration band was affected by the breaking of the hydrogen bonding network in the first and second hydration layers of the cations due to the presence of ClO_4^- ions.

We attempted to fit the envelope of the water bands as a function of WSR but did not get satisfactory results. However, the relative intensity ratios of the two shoulders at the lower wavenumber side (C_1 and C_2) to the main peak (water monomers) show an interesting dependence on the WSR, as illustrated in Figure 6. In the $NaClO_4$ droplets, the intensity ratio of the peaks at 3440 cm^{-1} (C_2) and at 3549 cm^{-1} (water monomers) (I_{3440}/I_{3549}) decreased linearly with a decrease in the molar ratio of H_2O/ClO_4^- (or WSR) until 6, where a steeper decrease of the ratio occurred. Similar transitions of the intensity ratios were observed for $LiClO_4$ (I_{3455}/I_{3553}) and $Mg(ClO_4)_2$ (I_{3411}/I_{3546}) droplets at a molar ratio of H_2O/ClO_4^- of about 7 and 8∼9, respectively. The same transition points were also observed with the intensity ratios of the C_1 component to the monomers, as shown in Figure 6.

Table 1 also shows the average residence time of a water molecule in the first hydration layer of the three cations.[34] Molecular dynamic simulations show that the residence times in the first hydration layer of Na^+ (9.9×10^{-12} s) and Li^+ (33×10^{-12} s) are about 2 and 7 times that of bulk solutions [$(4.6 \pm 0.3) \times 10^{-12}$ s]. The residence time of a water molecule in the first hydration layer of Mg^{2+} is about 6 orders larger than that in bulk water. This is why the coordination number in the first hydration layer of Mg^{2+} has been consistently found to be six in the literature, whereas those of Na^+ and Li^+ have been found to vary from 3 to 6, depending on its concentration and counterions.[32] If we use $M(H_2O)_m(H_2O)_n(H_2O)_k$ to represent a metal cation M with m, n, and k water molecules in the first and second hydration layers and in the neighborhood surrounding the second hydration layer, then $m = 6$ and $n = 12$ for Mg^{2+}; that is, 12 water molecules as donors of lone-pair electrons are needed in the second hydration layer to form full hydrogen bonds with the 6 water molecules in the first hydration layer. Such structures ($Mg^{2+}(H_2O)_{18}$) have been studied by Pye and Rudolph with ab initio method.[33] In Figure 6, the transition point of I_{3411}/I_{3546} of the spectra of $Mg(ClO_4)_2$ occurs at the molar ratio of H_2O/ClO_4^- of 8∼9 (or WSR = 16∼18), when the solvent-separated ion pairs start to form as discussed above. The replacement of the second-hydration-layer water molecules by ClO_4^- ions at WSR lower than 16∼18 results in the formation of solvent-separated ion pairs, and destroys the hydrogen bonding of water molecules between the first and second hydration layers. Thus, the initial linear trend of the intensity ratio in Figure 6 is attributed to the breaking of the hydrogen bonds in the second hydration layer by ClO_4^-. The second linear trend is attributed to the formation of the inner sphere solvent-separated ion pairs, which is a result of the breaking of the hydrogen bonding in the inner layer by ClO_4^-.

In 8 mol L^{-1} bulk $NaClO_4$ (WSR = 7) aqueous solutions, solvent-separated ion pairs and contact ion pairs are already present at mole fractions of 0.64 and 0.15, respectively.[26] However, the transition point of I_{3440}/I_{3549} was observed at WSR = 6 in $NaClO_4$ droplets, suggesting that the transition was not due to the formation of solvent-separated ion pairs and contact ion pairs. In fact, the residence time of water molecules in the first hydration layer of Na^+ is not much larger than that in bulk. Hence, the m hydrated water molecules in $Na^+(H_2O)_m(H_2O)_n(H_2O)_k$ are dynamically similar to the bulk water molecules. The formation of contact ion pairs between Na^+ and ClO_4^- weakens the hydration ability of the Na^+ and thus reduces the residence time of its hydrated water molecules further, making the water molecules in the first layer of Na^+ similar to bulk water molecules. Furthermore, m is reduced with the decrease of WSR when contact ion pairs are formed. Thus, the transition of I_{3440}/I_{3549} cannot be attributed to the presence of Na^+ but is a result of the structure breaking effect of ClO_4^- on hydrogen bonding, similar to that in the bulk.

The residence time of the water molecules in the first layer of Li^+ is higher than that of Na^+ but is much lower that that of Mg^{2+}, whereas the hydration energy of Li^+ is (-514.1 kJ mol^{-1}) slightly higher than that of Na^+ (-405.4 kJ mol^{-1}) but much smaller than that of Mg^{2+} (-1922.1 kJ mol^{-1}). Thus, the transition point of I_{3455}/I_{3553} or I_{3275}/I_{3553} for $LiClO_4$ droplets is intermediate between those of Na^+ and Mg^{2+} and was observed at WSR = 7.

IV. Conclusions

The use of an EDB to levitate supersaturated droplets has facilitated the study of the structures of water molecules. At very low WSR (e.g., 1.6 in $NaClO_4$ droplets), the υ_{O-H} bands (at 3549 and 3587 cm^{-1}) for water monomers with one and two weakly hydrogen bonds with ClO_4^- were observed even at room temperature. The polarization effect of the metal ions has led to a red shift in the peaks of water monomers, in the order of $Mg^{2+} > Li^+ > Na^+$. We have demonstrated that the intensity ratios of the peaks of the strong hydrogen bonds components (C_1 and C_2) to the water monomers are useful in studying the structure breaking effect of perchlorate on the hydrogen bond network of water in the hydration layers of metal ions.

Acknowledgment. Financial support from the Hong Kong RGC Earmarked Grant (HKUST6042/01P), the HKUST PDF grant, the National Natural Science Foundation of China (No. 20073004), and the Trans-Century Training Program Foundation for the Talents of Humanities and Social Science by the State Education Commission are gratefully acknowledged.

References and Notes

(1) Charlson, R. J.; Schwartz, S. E.; Hales, J. M.; Cess, R. D.; Coakley, J. A., Jr.; Hansen, J. E.; Hofman, D. J. *Science* **1992**, *255*, 423.
(2) Ha, Z.; Chan, C. K. *Aerosol Sci. Technol.* **1999**, *31*, 154.
(3) Chan, C. K.; Ha, Z.; Choi, M. Y. *Atmos. Environ.* **2000**, *34*, 4795.
(4) Zhang, Y. H.; Chan, C. K. *J. Phys. Chem. A* **2000**, *104*, 9191.
(5) Zhang, Y. H.; Chan, C. K. *J. Phys. Chem. A* **2002**, *106*, 285.
(6) (a) Keutsch, F. N.; Saykally, R. J. *P. Natl. Acad. Sci. U.S.A.* **2001**, *98* (19), 10533. (b) Keutsch, F. N.; Fellers, R. S.; Brown, M. G.; Viant, M. R.; Petersen, P. B.; Saykally, R. J. *J. Am. Chem. Soc.* **2001**, *123*, 5938.
(7) Bellissent-Funel, M. C.; Dore, J. C. *Hydrogen Bond Networks*, *NATO ASI Series, Series C: Mathematical and Physical Sciences*; Kluwer Academic Publishers: Dordrecht, The Netherlands, 1994; Vol. 435.
(8) Walrafen, G. E. *J. Chem. Phys.* **1970**, *52*, 4176.
(9) Ratcliffe, C. I.; Irish, D. E. *Can. J. Chem.* **1984**, *62*, 1134.
(10) Walrafen, G. E.; Hokmabadi, M. S.; Yang, W.-H. *J. Chem. Phys.* **1986**, *85*, 6964.
(11) Falk, M.; Ford, T. A. *Can. J. Chem.* **1966**, *44*, 1699.
(12) Hartman, K. A. *J. Phys. Chem.* **1966**, *70*, 270.
(13) Wyss, H. R.; Falk, M. *Can. J. Chem.* **1970**, *48*, 607.
(14) Senior, W. A.; Verrall, R. E. *J. Phys. Chem.* **1969**, *73*, 4242.
(15) Carey, D. M.; Korenowski, G. M. *J. Chem. Phys.* **1998**, *108*, 2669.
(16) Ikushima, Y.; Hatakeda, K.; Saito, N.; Arai, M. *J. Chem. Phys.* **1998**, *108*, 5855.
(17) Mitterböck, M.; Fleissner, G.; Hallbrucker, A.; Mayer, E. *J. Phys. Chem. B* **1999**, *103*, 8016.
(18) Kanno, H.; Hiraishi, J. *Chem. Phys. Lett.* **1981**, *83*, 452.
(19) Zangmeister, C. D.; Pemberton, J. E. *J. Phys. Chem. A* **2001**, *105*, 3788.
(20) (a) Tian, Z. Q.; Chen, Y. X.; Mao, B. W.; Li, C. Z.; Wang, J.; Liu, Z. F. *Chem. Phys. Lett.* **1995**, *240*, 224. (b) Zou, S. Z.; Chen, Y. X.; Mao, B. W.; Ren, B.; Tian, Z. Q. *J. Electroanal. Chem.* **1997**, *424*, 19. (c) Chen, Y. X.; Tian, Z. Q. *Chem. Phys. Lett.* **1997**, *281*, 379.
(21) (a) Choi, M. Y.; Chan, C. K. *J. Phys. Chem. A* **2002**, *106*, 4566. (b) Peng, C.; Chan, M. N.; Chan, C. K. *Environ. Sci. Technol.* **2001**, *35*, 4495. (c) Choi, M. Y.; Chan, C. K. *Environ. Sci. Technol.* **2002**, *36*, 2422.
(22) Schweiger, G. In *Analytical Chemistry of Aerosols*; Spurny, K. R., Ed.; CRC Press: Boca Raton, FL, 1999; pp 319−352.
(23) (a) Willard, H. H.; Smith, G. F. *J. Am. Soc. Chem.* **1923**, *45*, 286. (b) Lepeshkov, I. N.; Orekhov, O. L. *Sb. Tr. Yarosl. Gos. Ped. Inst.* **1969**, *66*, 62. (c) Lorimer, J. W. *Solubility Data Series*; Chan, C.Y., Ed.; *Alkaline Earth Metal Perchlorates*, IUPAC; Pergamon Press: Oxford, U.K., 1989; Vol. 41, p 14.
(24) Klassen, B.; Aroca, R.; Nazri, G. A. *J. Phys. Chem.* **1996**, *100*, 9334.
(25) Miller, A. G.; Macklin, J. W. *J. Phys. Chem.* **1985**, *89*, 1193.
(26) Frost, R. L.; James, D. W.; Appleby, R.; Mayes, R. E. *J. Phys. Chem.* **1982**, *86*, 3840.
(27) Blackburn, A. C.; Gallucci, J. C.; Gerkin, R. E.; Reppart, W. J. *Acta Crystallogr., Sect. C* **1993**, *C49*, 1437.
(28) Sequeira, A.; Bernal, I. D.; Faggiani, R. *Acta Cryst.* **1975**, *B31*, 1735.
(29) Joesten, M. D.; Drago, R. S. *J. Am. Chem. Soc.* **1962**, *84*, 3817.
(30) Perelygin, I. S.; Safiullina, N. R. *Zhurn. Struktur. Khimii.* **1967**, *8*, 205.
(31) Shcherba, L. D.; Sukhotin, A. M. *Zhurn. Fiz. Khimii.* **1959**, *33*, 2401.
(32) (a) Burgess, J. *Metal Ions in Solutions*; Ellis Horwood Limited: Sussex, U.K., 1978; pp 137−147. (b) Ryss, A. M.; Radchenko, I. V. *Zhurn. Struktur. Khimii.* **1965**, *6*, 182. Dorosh, A. K. *Strucure of Condensed System*; Vishcha shk.: Kiev, 1981; p 176. Palinkas, G.; Radnai, T.; Hajdu, F. *Z. Naturforsch. A.* **1980**, *35*, 107. (c) Chizhik, V. I. *Thermodynamics of Solvation*; Presses, IKHTI: Ivanovo, 1983; pp 6−7. (d) Glasstone, S. *Textbook of Physical Chemistry*, 2nd ed.; Macmillan: New York, 1956; p 921. Remy, H. *Trans. Faraday Soc.* **1927**, *23*, 381. Bourion, F.; Hun, O. *Hebd. Seanc. Acad. Sci. Paris* **1934**, *198*, 1921. Rutgers, A. T.; Hendikx, Y. *Trans. Faraday Soc.* **1962**, *58*, 2184. (e) Fratiello, A.; Lee, R. E.; Schuster, R. E. *Inorg. Chem.* **1970**, *9*, 82. Padova, I. *J. Chem. Phys.* **1963**, *39*, 2599. Padova, I. *J. Chem. Phys.* **1964**, *40*, 691. Nightingale, E. R. *J. Phys. Chem.* **1959**, *63*, 1381.
(33) (a) Rudolph, W.; Brooker, M. H.; Pye, C. C. *J. Phys. Chem.* **1995**, *99*, 3793. (b) Pye, C. C.; Rudolph, W.; Poirier, R. A. *J. Phys. Chem.* **1996**, *100*, 601. (c) Pye, C. C.; Rudolph, W. W. *J. Phys. Chem. A* **1998**, *102*, 9933.
(34) Ohtaki, H. *Monatsh. Chem.* **2001**, *132*, 1237.